INSTITUTE OF PHYSICS PUBLISHING CLASSICAL AND QUANTUM GRAVITY

Class. Quantum Grav. **20** (2003) 729–754 PII: S0264-9381(03)55685-4

On 'many-black-hole' vacuum spacetimes

Piotr T Chruściel[1,3] **and Rafe Mazzeo**[2]

[1] Albert Einstein Institute, Golm, Germany
[2] Department of Mathematics, Stanford University, Stanford, CA 94305, USA

E-mail: piotr@gargan.math.univ-tours.fr and mazzeo@math.stanford.edu

Received 6 November 2002
Published 3 February 2003
Online at stacks.iop.org/CQG/20/729

Abstract

We analyse the horizon structure of families of spacetimes obtained by evolving initial data sets containing apparent horizons with several connected components. We show that under certain smallness conditions the outermost apparent horizons will also have several connected components. We further show that, again under a smallness condition, the maximal globally hyperbolic development of the many-black-hole initial data constructed in Chruściel and Delay (2002 *Class. Quantum Grav.* **19** L71–9), or of the hyperboloidal data of Isenberg *et al* (2002 *Commun. Math. Phys.* **231** 529–68), will have an event horizon, the intersection of which with the initial data hypersurface is not connected. This justifies the *'many-black-hole'* character of those spacetimes.

PACS number: 04.70.Bw

1. Introduction

There is an ongoing effort to construct 'many-black-hole' solutions of the vacuum Einstein equations numerically (see, e.g. [2, 27, 28] and references therein). In practice this means that one numerically evolves initial data which contain trapped surfaces for as long as the computer allows. The question then arises whether the resulting spacetime does indeed contain more than one black hole, or for that matter, any. Several issues arise here.

(a) The notion of a black hole is usually tied to the existence of a conformal completion of the spacetime (but see [8] for alternative proposals). It is far from clear that the vacuum solutions, which are, in principle, associated with their numerical counterparts discussed in [2, 27, 28], possess sufficiently controlled conformal completions, if any.

(b) Even assuming the issues in point (a) do not occur, consider an initial data set $(\mathscr{S}, g, K)$ which contains several trapped, or marginally trapped, surfaces[4]. If yet another trapped or

[3] Permanent address: Département de mathématiques, Faculté des Sciences, Parc de Grandmont, F37200 Tours, France.

[4] There sometimes exist Cauchy hypersurfaces in spacetimes containing black holes which do not contain any compact trapped surfaces [34], but this is irrelevant to our considerations here.

 © 2003 IOP Publishing Ltd Printed in the UK

marginally trapped surface S_0 encloses all the previous ones, then the geometry enclosed by S_0 is hidden from external observers by the null hypersurface $\dot{J}^+(S_0)$. Numerical calculations of tentative radiation patterns inside $J^+(S_0)$ have absolutely no relevance to the data detected at $\mathscr{I}^+$. Thus *if* one is willing to associate black-hole regions with apparent horizons, then only the outermost apparent horizons are relevant. In this context, a condition for a multi-black-hole spacetime would be that the *outermost* apparent horizon has more than one component.

(c) In any case, the event horizon itself might have nothing to do with the apparent horizons, even the outermost ones. Under appropriate hypotheses, the existence of an apparent horizon implies the existence of a black-hole region, but this can be much larger than the region enclosed by the outermost apparent horizon. In particular, one might imagine a situation in which the outermost apparent horizon has several components, all of which are enclosed by a connected event horizon, so that the spacetime contains only a single black-hole region.

The object of this paper is to point out that the issues raised above can be analysed in a reasonably satisfactory way for the 'many Schwarzschild' initial data constructed in [9], or for the data obtained by the gluing constructions of [21, 23], or for families of initial data sharing certain qualitative properties, as made precise below, similar to those of [9, 21]. The first main result here is that for a rather general class of 'small-data' families of black-hole spacetimes, the outermost apparent horizon $\mathscr{A}$ will have several connected components. We prove this both on the usual asymptotically flat initial data hypersurfaces and on hyperboloidal ones. For the initial data of [9] the relevant smallness condition holds when the mass parameters m_i, $i = 1, \ldots, I$, of the individual Schwarzschild black holes are small enough as compared to the distance parameters r_i. For the initial data of [21] the smallness condition holds when the gluing necks are sufficiently small.

One of the features of the initial data sets of [9] is that these metrics are *exactly* Schwarzschild outside a compact set, and this guarantees that for any one of these, the associated maximal globally hyperbolic development $(\mathscr{M}, g)$ necessarily has a $\mathscr{I}^+$ which is complete to the past[5]. As already indicated, the existence of $\mathscr{I}^+$ is the usual starting point for a discussion of black-hole regions. The second main result here is the proof that, for certain configurations and again for small enough mass parameters, the intersection

$$\mathscr{E}^+_{\mathscr{S}} := \dot{J}^-(\mathscr{I}^+) \cap \mathscr{S} \tag{1.1}$$

of the future event horizon $\dot{J}^-(\mathscr{I}^+)$ with the initial data hypersurface $\mathscr{S}$ has at least I components. (Indeed, we show that $\mathscr{A}$ has *exactly* I components and believe that this should also be true for $\mathscr{E}^+_{\mathscr{S}}$; a proof of such a claim about $\mathscr{E}^+_{\mathscr{S}}$ would require complete control of the global structure of the resulting spacetime, which is well beyond the range of techniques available nowadays.)

2. 'Many-black-hole' initial data

There are several constructions of families of initial data containing apparent horizons, see [1, 3, 4, 14] and references therein. In this section, we briefly describe three such families of 'many-black-hole initial data'. Before doing this, it is useful to recall how apparent horizons

[5] We note that both here, and in several situations of interest, one can use the results in [24] to infer the existence and past-completeness of $\mathscr{I}^+$. However, the estimates there are based on spherical outgoing null hypersurfaces, which can be used to prove the existence of, at best, a connected black-hole region (if any). Further, the differentiability properties of $\mathscr{I}^+$ which can be directly inferred from that work (compare [7]) are not sufficient to invoke the stability results of [16], as needed below.

are detected using initial data (compare [4]): let, thus, $(\mathscr{S}, g, K)$ be an initial data set, and let $S \subset \mathscr{S}$ be a compact embedded two-dimensional two-sided submanifold in $\mathscr{S}$. If n^i is the field of outer normals to S and H is the outer mean extrinsic curvature[6] of S within $\mathscr{S}$ then, in a convenient normalization, the divergence θ_+ of future-directed null geodesics normal to S is given by

$$\theta_+ = H + K_{ij}(g^{ij} - n^i n^j). \tag{2.1}$$

In the time-symmetric case θ_+ reduces thus to H, and S is trapped if and only if $H < 0$, marginally trapped if and only if $H = 0$. In the hyperboloidal case with $K_{ij} = g_{ij}$ we obtain $\theta_+ = H + 2$.

2.1. *Brill–Lindquist initial data*

Probably the simplest examples are the time-symmetric initial data of Brill and Lindquist. Here, the space-metric at time $t = 0$ takes the form

$$g = \psi^4(\mathrm{d}x^2 + \mathrm{d}y^2 + \mathrm{d}z^2), \tag{2.2}$$

with

$$\psi = 1 + \sum_{i=1}^{I} \frac{m_i}{2|\vec{x} - \vec{x}_i|}.$$

The positions of the poles $\vec{x}_i \in \mathbb{R}^3$ and the values of the mass parameters $m_i \in \mathbb{R}$ are arbitrary. If all the m_i are positive and sufficiently small, then there exists a small minimal surface with the topology of a sphere which encloses $\vec{x}_i$. This follows from general arguments in geometric measure theory, as implemented and described in more detail in section 3. In addition, from [24], the associated maximal globally hyperbolic development possesses a $\mathscr{I}^+$ which is complete to the past, but the differentiability properties of the conformally completed metric may not be sufficient to justify some key steps of the global analysis below concerning event horizons.

2.2. *The 'many Schwarzschild' initial data of [9]*

There is a well-known special case of (2.2), which is the space-part of the Schwarzschild metric centred at $\vec{x}_0$ with mass m:

$$g = \left(1 + \frac{m}{2|\vec{x} - \vec{x}_0|}\right)^4 \delta, \tag{2.3}$$

where δ is the Euclidean metric. Abusing terminology in a standard way, we call (2.3) simply the Schwarzschild metric. Allowing the mass parameter to be nonpositive leads to naked singularities or flat regions but we shall always require positive masses here. The sphere $|\vec{x} - \vec{x}_0| = m/2$ is minimal, and the region $|\vec{x} - \vec{x}_0| < m/2$ corresponds to the second asymptotic region, beyond the Einstein–Rosen bridge.

Now fix the radii $0 \leqslant 4R_1 < R_2 < \infty$. Denoting by $B(\vec{a}, R)$ the open coordinate ball centred at $\vec{a}$ with radius R, choose points

$$\vec{x}_i \in \Gamma_0(4R_1, R_2) := \begin{cases} B(0, R_2) \backslash \overline{B(0, 4R_1)}, & R_1 > 0 \\ B(0, R_2), & R_1 = 0, \end{cases}$$

[6] We use the convention that gives $H = 2/r$ for round spheres of radius r in three-dimensional Euclidean space.

and radii r_i, $i = 1, \ldots, 2N$, so that the closed balls $\overline{B(\vec{x}_i, 4r_i)}$ are all contained in $\Gamma_0(4R_1, R_2)$ and are pairwise disjoint. Set

$$\Omega := \Gamma_0(R_1, R_2) \backslash \big(\cup_i \overline{B(\vec{x}_i, r_i)} \big). \tag{2.4}$$

We assume that the $\vec{x}_i$ and r_i are chosen so that Ω is invariant with respect to the reflection $\vec{x} \to -\vec{x}$. Now consider a collection of non-negative mass parameters, arranged into a vector as

$$\vec{M} = (m, m_0, m_1, \ldots, m_{2N}),$$

where $0 < 2m_i < r_i$, $i \geqslant 1$, and, in addition, with $2m_0 < R_1$ if $R_1 > 0$ but $m_0 = 0$ if $R_1 = 0$. We assume that the mass parameters associated with the points $\vec{x}_i$ and $-\vec{x}_i$ are the same. The remaining entry m is explained below.

Given this data, it follows from the work of [13] (as pointed out in [9], compare [10]) that there exists a $\delta > 0$ such that if

$$\sum_{i=0}^{2N} |m_i| \leqslant \delta, \tag{2.5}$$

then there exists a number

$$m = \sum_{i=0}^{2N} m_i + O(\delta^2)$$

and a C^∞ metric $\hat{g}_{\vec{M}}$ which is a solution of the time-symmetric vacuum constraint equation

$$R(\hat{g}_{\vec{M}}) = 0,$$

such that

1. on the punctured balls $B(\vec{x}_i, 2r_i)\backslash\{\vec{x}_i\}$, $i \geqslant 1$, $\hat{g}_{\vec{M}}$ is the Schwarzschild metric, centred at $\vec{x}_i$, with mass m_i;
2. on $\mathbb{R}^3 \backslash \overline{B(0, 2R_2)}$, $\hat{g}_{\vec{M}}$ agrees with the Schwarzschild metric centred at 0, with mass m;
3. if $R_1 > 0$, then $\hat{g}_{\vec{M}}$ agrees on $B(0, 2R_1)\backslash\{0\}$ with the Schwarzschild metric centred at 0, with mass m_0.

In fact, this construction also gives that $\hat{g}_{\vec{M}}$ is symmetric under the parity map $\vec{x} \to -\vec{x}$.

2.3. Black holes and gluing methods

A recent alternative technique for gluing initial data sets is given in [21]; see also [23] for the time-symmetric case and [22] for more general results in the asymptotically Euclidean case. In this approach, general initial data sets on compact manifolds or with asymptotically Euclidean or hyperboloidal ends are glued together to produce solutions of the constraint equations on the connected sum manifolds. Only very mild restrictions on the original initial data are needed. The neck regions produced by this construction are again of Schwarzschild type. The overall strategy of the construction is similar to that used by Corvino (and in many previous gluing constructions). Namely, one takes a family of approximate solutions to the constraint equations and then attempts to perturb the members of this family to exact solutions. There is a parameter η which measures the size of the neck, or gluing region; the main difficulty is caused by the tension between the competing demands that the approximate solutions become more nearly exact as $\eta \to 0$ while the underlying geometry and analysis become more singular. In this approach, the conformal method of solving the constraints is used, and the solution involves a conformal factor which is exponentially close to 1 (as a function of η) away from the neck region, but which is nonetheless not completely localized.

Consider first an asymptotically flat time-symmetric initial data set, to which several other time-symmetric initial data sets have been glued by this method. If one assumes that the resulting necks are mean outer convex, as described in detail in section 3,[7] then the existence of a nontrivial minimal surface, hence of an apparent horizon, follows by standard results, cf section 3. This implies the existence of a (possibly disconnected) black-hole region in the maximal globally hyperbolic development of the data. As for the Brill–Lindquist construction, the asymptotically flat initial data produced in this way may not have sufficient differentiability at the resulting $\mathscr{I}^+$ to obtain good information about $\mathscr{C}^+_{\mathscr{I}}$.

Consider, next, hyperboloidal initial data with

$$K_{ij} = g_{ij}. \tag{2.6}$$

It follows from (2.1) that in this setting trapped or marginally trapped surfaces are characterized by the condition

$$\theta_+ = H + 2 \leqslant 0. \tag{2.7}$$

Fixing a polar coordinate r on the standard three-dimensional hyperboloid, the constant curvature -1 metric takes the form

$$g = \frac{1}{r^2+1}\,\mathrm{d}r^2 + r^2\,\mathrm{d}\Omega^2$$

(where $\mathrm{d}\Omega^2$ is the constant curvature +1 metric on S^2), then it is straightforward to calculate that the mean curvature with respect to the outer normal of the 'constant r' geodesic spheres is given by the formula

$$H = 2\sqrt{1+r^{-2}}.$$

Now, suppose we glue together two hyperboloidal initial data sets. From the point of view of far away observers sitting on the other side of the ensuing neck, the inner-pointing normal for a geodesic sphere on one half of this configuration is actually pointing towards them, thus outer-pointing as far as they are concerned; hence the quantity

$$-H + 2 = -2/\left(r^2 + \sqrt{r^2+1}\right)$$

measures 'trapedness' with respect to the other asymptotic region. This is negative for any $r > 0$ on the hyperboloid, and will remain strictly negative when r is large enough even after the gluing has been performed. This means that large spheres on one side of the neck are trapped from the point of view of the $\mathscr{I}^+$ on the other side and hence, by standard Lorentzian geometry arguments, cannot be seen from that Scri. This again implies the existence of a black-hole region. Note that this simplest case is rotationally invariant, and there is a unique minimal sphere encircling the neck (see lemma 3.4). Hence by continuity, there is at least one marginally trapped, i.e. with $\theta_+ = 0$, rotationally symmetric geodesic sphere. A similar argument establishes the existence of black-hole regions when several initial data sets satisfying (2.6), at least two of which are hyperboloidal, are glued together.

3. Outermost apparent horizons with many components

In this section, we generalize the examples above and consider a family of asymptotically Euclidean metrics $\{g_\eta\}$, $0 < \eta \leqslant \eta_0$, which satisfy the two properties below. Our goal is to show that when η_0 is sufficiently small, the outermost apparent horizon of each of these metrics has a large number of components.

[7] This will hold if the gluing regions are made small enough.

We assume that for $\eta \in (0, \eta_0]$, $(\mathscr{S}, g_\eta)$ is a Riemannian manifold with a boundary of dimension 3, with a single asymptotically Euclidean end E, and such that $\partial\mathscr{S}$ is a union of I copies of S^2. (In the context of the initial data of section 2.2, this amounts to removing from the manifold that part which lies on the other side of the connecting necks.) We suppose furthermore that around each boundary component there is an annular 'neck region' $A_i, i = 1, \ldots, I$, equipped with a diffeomorphism $\Phi_i : S^2 \times [-1, 1] \to A_i$, such that $\Phi_i(S^2 \times \{-1\}) = (\partial\mathscr{S}) \cap A_i$. Thus,

$$\mathscr{S} = E(\eta) \cup A_1 \cup \cdots \cup A_I$$

is a union of manifolds with boundary, intersecting only along the submanifolds $(\partial E(\eta)) \cap A_i = \Phi_i(S^2 \times \{+1\})$ so that the A_i are mutually disjoint. We call $\Phi_i(S^2 \times \{-1\})$ and $\Phi_i(S^2 \times \{+1\})$ the outer and inner boundaries of A_i. The end $E(\eta)$ is diffeomorphic to an exterior region in $\mathbb{R}^3$, and we fix a family of diffeomorphisms

$$\Psi_\eta : \mathbb{R}^3 \setminus \cup_i B(\vec{x}_i, \rho_i(\eta)) \longrightarrow E(\eta),$$

and assume that the radii of these balls $\rho_i(\eta)$ tend to 0 as $\eta \searrow 0$. (It is only a matter of convention that we think of the annular regions as fixed, whereas $E(\eta)$ is identified with an η-dependent region. However, the metric g_η varies nontrivially on each of these regions.)

Our hypotheses on the metrics g_η are as follows:

(a) *Metric convergence on the distinguished end.* If K is any compact subset of $\mathbb{R}^3 \setminus \cup_i \{\vec{x}_i\}_{i=1,\ldots,I}$, then for some $\alpha \in (0, 1)$

$$\lim_{\eta \to 0} \|\Psi_\eta^*(g_\eta) - \delta\|_{C^{2,\alpha}(K)} = 0;$$

here δ is the Euclidean metric on $\mathbb{R}^3$.

(b) *Mean outer convex necks and small minimizing cycles.* For η in a sufficiently small interval $(0, \eta_0)$, both the inner and outer boundaries $\Phi_i^{-1}(S^2 \times \{\pm 1\})$ of A_i are mean outer convex with respect to g_η; furthermore, there exists a smoothly embedded sphere S_i which represents the fundamental class $\sigma_i \in H_2(A_i, \mathbb{Z})$ and with area $|S_i| \to 0$ as $\eta \to 0$.

Each of the three constructions outlined in section 2.2 produces families of metrics satisfying these hypotheses. For example, for the construction in section 2.2, if $\vec{M}_0 := (m_0, m_1, \ldots, m_{2N})$ is a $(2N+1)$-tuple of non-negative numbers and $\vec{M}(\eta) = (m(\eta), \eta\vec{M}_0)$ is the associated mass-parameter vector from that construction, then $g_\eta := \hat{g}_{\vec{M}(\eta)}$ satisfies both these hypotheses. Similarly, the initial data of section 2.3 satisfy the hypotheses here if η is a sufficiently small parameter controlling the outer radii of the I necks across which the gluing is performed.

We begin with a geometric result which holds under slightly more general hypotheses.

Lemma 3.1. *Let g be a Riemannian metric on $A = S^2 \times [-1, 1]$ such that the two boundaries $S^2 \times \{\pm 1\}$ are mean outer convex. Fix a generator σ_A for $H_2(A, \mathbb{Z})$. Then any surface Σ which is absolutely area minimizing in this homology class is smoothly embedded, lies in the interior of A and consists of a single component of multiplicity one.*

Proof. The existence of a homological area-minimizer Σ in the class of integral currents in a manifold with mean outer convex boundaries, and the regularity of its support, is a standard result in geometric measure theory, cf [32, theorems 37.2 and 37.7]. (These arguments work equally well for domains with mean outer convex boundaries, cf [31], and by the maximum principle, the support of the resulting minimizer is disjoint from ∂A.) In particular, the support

of Σ is a finite union of smooth, oriented, connected surfaces $\Sigma_1, \ldots, \Sigma_J$, where each Σ_j appears with some non-vanishing integer multiplicity k_j. Thus, on the level of homology

$$k_1[\Sigma_1] + \cdots + k_J[\Sigma_J] = \sigma_A,$$

whereas

$$|\Sigma| = |k_1||\Sigma_1| + \cdots + |k_J||\Sigma_J|. \tag{3.1}$$

We claim that the support of Σ has only one component, and this occurs with multiplicity 1. To prove this, note first that any component Σ_j divides $S^2 \times [-1, 1]$ into precisely two components. This may be seen by 'capping off' the boundary $S^2 \times \{-1\}$ of A by adding a 3-ball; the interior of the resulting manifold $A \cup B^3$ is diffeomorphic to $\mathbb{R}^3$. By the Jordan separation theorem, any smooth, oriented, connected surface Σ_j embedded in A, hence in $\mathbb{R}^3$, divides this space into an 'inside' and an 'outside'. For example, a point p lies in the inner component if (all) generic paths γ connecting p to the outer boundary $S^2 \times \{1\}$ intersect Σ_j an odd number of times. In any case, this decomposition shows that in homology, $[\Sigma_j] = \pm\sigma_A$ or else $[\Sigma_j] = 0$ for each j. If any Σ_j is null-homologous, then we can obviously discard it, since it adds a positive amount to the area of Σ without contributing to the homology class; possibly changing orientations, we can therefore assume that each $[\Sigma_j] = \sigma_A$.

Finally, amongst the Σ_j select one, Σ', with smallest area. Then from (3.1), $|\Sigma'| \leqslant |\Sigma|$, and equality holds only if Σ' is the only component, and occurs with multiplicity 1. Thus Σ' is the connected homological area-minimizer, as required. □

Now, let us return to the more general situation. Using this lemma, we represent the generator $\sigma_j = [\Phi_j\,(S^2 \times \{+1\})]$ of $H_2(A_j, \mathbb{Z})$ by a homologically area-minimizing surface Σ_j; according to hypothesis (b), σ_j is also represented by the sphere S_j. Both Σ_j and S_j are smoothly embedded, connected surfaces of multiplicity 1. (Since g_η has non-negative scalar curvature, it is known [5, 31] that Σ_j—or indeed any stable minimal surface—must be either a sphere S^2 or possibly a torus T^2 if g_η is flat in a neighbourhood of Σ_j.) By assumption, $|S_j| \to 0$, and hence $|\Sigma_j| \to 0$ as well.

It is proved in [20, lemma 4.1] that with the hypotheses above, for every $0 < \eta \leqslant \eta_0$ there exists a unique outermost minimal surface S_η, which is a union of embedded stable minimal spheres of class $C^{k+1,\alpha}$ if g_η is of class $C^{k,\alpha}$. Furthermore, if we denote by $\mathscr{S}'$ the exterior of S_η in $\mathscr{S}$ (i.e. the unbounded component of $\mathscr{S} \backslash S_\eta$), then S_η is absolutely area minimizing in its homology class in $\mathscr{S}'$ and, moreover, $\mathscr{S}'$ is simply connected.

Theorem 3.2. *There exists $\eta_1 \in (0, \eta_0]$ such that if $\eta \in (0, \eta_1]$, then $S_\eta \subset \cup_{i=1}^I A_i$ and the intersection of S_η with each annular region A_i is non-empty. Hence, S_η has at least I connected components. If we assume that there do not exist any stable minimal homologically trivial surfaces in any of the regions (A_i, g_η) when η is small enough, then $S_\eta \cap A_i$ contains exactly one component, and hence S_η has precisely I components.*

Proof. Let $S(0, R)$ denote a large sphere in $\mathbb{R}^3$ which contains all of the points $\vec{x}_i$, and let Ω denote the part of $\mathscr{S}$ interior to this sphere. Coherently orienting the fundamental classes $\sigma_j(H_2(A_j, \mathbb{Z}))$, we have that $[S(0, R)] = \sigma := \sigma_1 + \cdots + \sigma_I$, where we regard $\sigma_j \in H_2(A_j, \mathbb{Z}) \hookrightarrow H_2(\mathscr{S}, \mathbb{Z})$, as induced by the inclusions $A_j \hookrightarrow \mathscr{S}$. From [20, lemma 4.1], we know that $\mathscr{S}'$ is diffeomorphic to the complement of a finite number of spheres in $\mathbb{R}^3$, and hence S_η must be homologous to $S(0, R)$ as well, i.e. $[S_\eta] = \sigma$. For each η we choose area-minimizing representatives $\Sigma_j(\eta)$ of σ_j in A_j, as in the preceding lemma. By hypothesis (a), $S(0, R)$ is mean outer convex for g_η if η is small enough, since it is strictly convex for the limiting Euclidean metric δ. Thus, we have

$$|\Sigma_1| + \cdots + |\Sigma_I| \leqslant |S_\eta| \leqslant |S(0, R)|.$$

The first inequality holds because $\cup\Sigma_i$ is absolutely area minimizing in its homology class in $\mathscr{S}$, while the second inequality follows from the fact that S_η is absolutely minimizing in its homology class in $\mathscr{S}'$. We claim that for η sufficiently small, S_η lies in the union $A_1 \cup \cdots \cup A_I$. Granting this claim for the moment, let us prove that S_η has at least I components. Choose for each j a smooth embedded curve γ_j which connects the inner boundary $\Phi_j\,(S^2 \times \{-1\})$ of A_j to $S(0, R)$, does not intersect any of the other annular regions A_i, $i \neq j$ and which represents the Poincaré dual of σ_j in $H_1(\Omega, \partial\Omega)$. Then, the homological intersection number of γ_j with $[S_\eta]$ equals

$$\langle [\gamma_j], \sigma \rangle = \langle [\gamma_j], \sigma_1 + \cdots + \sigma_I \rangle = 1.$$

On the other hand, if γ_j is in a general position, then this intersection number is also computed by counting the signed geometric intersections of this curve and this surface. Therefore, this geometric intersection is nontrivial, which shows that $S_\eta \cap A_j \neq \emptyset$ for each j, and hence S_η has at least I components.

To prove the claim, suppose there exists a sequence $\eta_\ell \to 0$ such that $S(\ell) := S_{\eta_\ell}$ contains a point $\vec{q}_\ell \in \Omega \backslash \cup A_i$ with $\vec{q}_\ell \to \vec{q} \in \mathbb{R}^3 \backslash \{\vec{x}_1, \ldots, \vec{x}_I\}$. The interior curvature estimate for embedded stable minimal surfaces proved by Schoen [30] states that there is a uniform upper bound for norm squared of the second fundamental form of $S(\ell)$ with respect to g_η near q_ℓ. More precisely, for any $\vec{p} \in S(\ell)$ with $\rho(\vec{p}) = \min_i\{|\vec{p} - \rho_i(\eta)|\} \geqslant \delta > 0$ for ℓ sufficiently large, there exists a constant $C > 0$, independent of ℓ, such that $|II_{S(\ell)}(p)|^2 \leqslant C$. By standard calculus, this implies that the portion of $S(\ell)$ in a ball of radius $\rho(\vec{p}/2)$ around $\vec{p}$ may be written as a graph with uniformly bounded gradient over a disc of radius $\rho(\vec{p})/4$ in $T_{\vec{p}}S(\ell)$. In particular, the area of $S(\ell)$ is uniformly bounded below by a positive constant.

Applying these bounds to a finite covering of $\Omega \backslash \cup_i B(\vec{x}_i, \rho)$ for any $\rho > 0$, and then taking a diagonal subsequence for some sequence $\rho_j \to 0$, we may extract a subsequence $S(\ell')$ which converges to a *nontrivial* smoothly embedded minimal surface $S(\infty)$ in $\mathbb{R}^3 \backslash \{\vec{x}_1, \ldots, \vec{x}_I\}$. Since all of the $S(\ell')$ are unions of spheres, and the number of components is uniformly bounded, the limiting surface must have finite genus. In addition, $S(\infty)$ is compact and has bounded area. We may now apply a well-known removable singularities theorem for minimal surfaces, see [6, proposition 1] for a proof, which shows that $S(\infty)$ is a nontrivial compact embedded minimal surface in $\mathbb{R}^3$. Since no such surfaces exist, we have reached a contradiction. We have now proved the first assertion, and hence that S_η has at least one connected component in each A_i.

For the remaining assertion, write $S_i(\eta) = S_\eta \cap A_i$, and suppose that this surface has more than one component for some i, i.e. $S_i(\eta) = \cup_{j=1}^J S_{ij}(\eta)$, where $J > 1$ and the $S_{ij}(\eta)$ are smooth embedded surfaces. By the same argument as in lemma 3.1, each $S_{ij}(\eta)$ separates A_i into two components. If A_i contains no null-homologous stable minimal surfaces, then each component of $A_i \backslash S_{ij}(\eta)$ must contain exactly one of the two boundaries $\Phi_i\,(S^2 \times \{\pm 1\})$. However, the components $S_{ij}(\eta)$ are disjoint, and so if there are at least two, then any one must be contained in either the interior or exterior region of another; since their union is an outermost surface this is impossible. We conclude that $S_i(\eta)$ is connected. This completes the proof. □

In the case of data of section 2.2 the hypotheses of the second part of theorem 3 are verified.

Corollary 3.3. *Let $I \in \mathbb{N}, \vec{M}_0 \in \mathbb{R}^I$ and consider initial data of section 2.2, with $\vec{M}(\eta) = (m(\eta), \eta\vec{M}_0)$ and $g_\eta := \hat{g}_{\vec{M}(\eta)}$. If η is small enough, then the outermost apparent horizon is precisely the union of the Schwarzschild horizons $|\vec{x} - \vec{x}_i| = m_i/2$.*

Proof. Let A_i be small annular regions around the $\vec{x}_i$, chosen so that the metric is exactly Schwarzschild there, then by theorem 3.2 we have $S_\eta \subset \cup_i A_i$ for small enough η. The result follows now from the following fact: □

Lemma 3.4. *The only compact embedded minimal surface in a Riemannian Schwarzschild metric (2.3) is the sphere* $|\vec{x} - \vec{x}_0| = m/2$.

Proof. The Riemannian Schwarzschild metric is foliated by spheres of constant mean curvature. These are outer mean convex with respect to the normal pointing away from the neck. We may now apply the maximum principle. If S is any compact embedded (or even immersed) minimal surface, then there is some such outermost sphere which makes 'first contact' with S, which is a contradiction. The only alternative is that S coincides with one of these spheres, and since it is minimal, it must be the central one.

We may also argue using Lorentzian methods. In fact, standard causality theory shows that a compact embedded minimal surface within a time symmetric Cauchy surface cannot be seen from $\mathscr{I}^+$, and so we may obtain the conclusion by inspecting the well-known conformal diagram for the Kruskal–Szekeres extension of the Schwarzschild spacetime. □

Using [20, lemma 4.1] one last time, each component of S_i is a sphere, and it is plausible that these must agree with the homologically area-minimizing surfaces $\Sigma_i \subset A_i$, whose topology is *a priori* either that of a sphere or a torus. In each of the examples in the last section, the annular regions A_i are small perturbations of rescalings of the Riemannian Schwarzschild metric, and so one may construct a foliation by constant mean curvature spheres using the implicit function theorem; from this it follows just as before that there is a unique stable minimal surface representing σ_i, so that $S_i' = \Sigma_i$ for all i. However, it is not clear that this is true in more general cases.

There is an analogue of theorem 3.2 concerning trapped surfaces for asymptotically hyperboloidal initial data sets. Suppose that $\mathscr{S}$ has the same topology as before, but that the metrics g_η are asymptotically hyperboloidal. Metrics of this sort, with many necks, can be constructed as in section 2.3. We suppose that the diffeomorphism Ψ_η^{-1} identifies $E(\eta)$ with the complement of a finite number of balls in $\mathbb{H}^3$ (or indeed any asymptotically hyperboloidal manifold with constant negative scalar curvature); we also replace the hypotheses (a) and (b) by

(a′) *Metric convergence on the distinguished end.* If K is any compact subset of $\mathbb{H}^3 \setminus \cup_i \{\vec{x}_i\}_{i=1,\dots,I}$, then for some $\alpha \in (0, 1)$

$$\lim_{\eta \to 0} \|\Psi_\eta^*(g_\eta) - g_{\mathscr{H}}\|_{C^{2,\alpha}(K)} = 0;$$

here $g_{\mathscr{H}}$ is the standard hyperbolic metric on $\mathbb{H}^3$.

(b′) *Neck boundaries with controlled mean curvature.* For η in a sufficiently small interval $(0, \eta_0)$, the outer boundaries Φ_i $(S^2 \times \{-1\})$ have mean curvature $h < -2$ (with respect to the inward-pointing unit normal).

We shall be using the maximum principle in the following form. Let S_1 and S_2 be two oriented, connected, embedded surfaces with constant mean curvature H_1 and H_2, respectively. Suppose that these surfaces are tangent at a point p and their normals are equal at this point, and that in some small neighbourhood S_1 lies on the 'interior' of S_2 (with respect to the normal). Then necessarily $H_1 \geqslant H_2$, and if $H_1 = H_2$, these surfaces must coincide. As a slightly weaker statement, if H_1 and H_2 are now possibly variable and if $H_1 > H_2$ everywhere, then this one-sided tangency cannot occur. As an immediate application, let Σ be any compact-oriented surface in $\mathbb{H}^3$ which contains all of the points $\vec{x}_i$ in its interior, and which has mean

curvature everywhere greater than -2 with respect to its outward normal. (For example, we could let $\Sigma = S(0, R)$, a large sphere.) This mean curvature remains greater than -2 when computed with respect to the metric g_η when η is small enough. Hence, S_η cannot be internally tangent to this sphere, and this shows that, in particular, S_η is contained in a fixed neighbourhood of the convex hull of the $\vec{x}_i$.

Proposition 3.5. *Under hypotheses (a′) and (b′), there is at least one (smooth, embedded, oriented) surface S_η which is homologous to $S(0, R) \subset \mathbb{H}^3$ (for sufficiently large R) and which has mean curvature -2 with respect to the normal pointing into the unbounded component of $\mathscr{S}\backslash S_\eta$, i.e. is marginally trapped.*

Proof. Since $\mathscr{S}$ is a manifold with boundary, the volume form $\mathrm{d}V_{g_\eta}$ is exact, hence equals $\mathrm{d}\Lambda$ for some (non-unique) 2-form Λ. Now, define the functional

$$L(S) = A(S) + \int_S \Lambda.$$

Note that changing Λ alters L by a constant in each homology class, but this is irrelevant to our purposes. This functional was studied, for example, in [35], and it follows from (2.14) in that paper that if S is a smooth stationary point of L, then the mean curvature of S is equal to -2.

Henceforth, let $S(0, R)$ denote any large geodesic sphere in $\mathbb{H}^3$ which encloses all of the points $\vec{x}_i$, and which we identify with a surface in $\mathscr{S}$ using Ψ_η. We may apply the usual geometric measure theory arguments, as follows, to conclude the existence of a smooth minimizer in the homology class of $S(0, R)$. First, it is clear that $L(S(0, R))$ increases without bound as $R \to \infty$. Next, when looking for a minimizer S, we may as well assume that S lies in the bounded component U of $\mathscr{S}\backslash S(0, R)$ for, if this were not the case, we could replace S by a homologous surface S' on which L assumes a smaller value. For example, if V is the bounded component of $\mathscr{S}\backslash S$, then $\partial(\overline{U \cap V})$ is a suitable[8] choice for S'. Hence, since we may assume that any minimizing sequence S_j remains within a compact set in $\mathscr{S}$, and since L is bounded below, we may find a minimizer S_η. The assumption that the outer boundaries have mean curvature $H < -2$ ensures that S_η remains in the interior of $\mathscr{S}$; cf [35 lemma 4]. The same regularity theory as was quoted earlier implies that the minimizer S_η is a smooth embedded and oriented surface in the interior of $\mathscr{S}$. □

Theorem 3.6. *Assume $(\mathscr{S}, g_\eta)$ is asymptotically hyperboloidal and satisfies the hypotheses (a′) and (b′). For η in some sufficiently small interval $(0, \eta_1]$, any trapped surface S_η which is homologous to $S(0, R)$ is contained in $\cup_{i=1}^{I} A_i$ and has at least I connected components.*

Note that we are not assuming that S_η is an outermost trapped surface here.

Proof. We have already indicated that such trapped surfaces exist. To prove that $S_\eta \subset \cup_i A_i$, we proceed as before and assume that this is not the case. To take a limit as $\eta \to 0$, we use the methods and estimates from [25, 26], which adapt in a straightforward way to small metric perturbations of hyperbolic space; cf also [35 Lemma 2]. In general, the situation is not as simple as for stable minimal surfaces because of the possibility of small necks in S_η pinching off, even in regions where the ambient geometry is uniform. One can prove that the limit surface S' is a finite union of smooth embedded surfaces S'_j which are mutually tangent at their points of intersection. (This part of the argument does not use specifically that $|H| = 2$,

[8] This follows from convexity: if one lets S_1 be the portion of S outside the sphere, and Π the projection from the exterior onto the surface of the sphere, then $\Pi(S_1)$ has less area than S_1, because the Jacobian of Π is everywhere less than 1. So the sphere contribution to L is reduced; clearly the volume contribution is reduced as well.

and it is possible one could use this special feature more strongly and show directly that S' is smooth; however, this is not so important for our purposes.) We may use the same removable singularities theorem as before, or rather its proof, to show that each S'_j is smooth at the points $\vec{x}_i$. However, each S'_j is compact and has constant mean curvature -2. But one could then find a horosphere tangent to S'_j, for example by bringing it in from infinity (in any direction) until it reaches a point of first contact, and this would contradict the maximum principle. Hence S'_j could not exist. (An alternative nonexistence proof is to note that if such S_j existed, then Minkowski spacetime would contain non-empty black-hole regions.)

We have now reduced to the case where $S_\eta \subset \cup A_i$. The same intersection theory argument as in the proof of theorem 3.2 shows that each of the intersections $S_\eta \cap A_i$ is non-empty, and so S_η must have at least I components. Note that each A_i contains an area-minimizing surface Σ_i which is homologous to the outer boundary, and the maximum principle implies that S_η is contained in the region between Φ_i $(S^2 \times \{-1\})$ and Σ_i. □

One can impose various geometric conditions on the metric g_η on the A_i which would ensure that S_η has exactly I components. A rather stringent one, which, however, is satisfied for the asymptotically hyperboloidal initial data sets of [21] for small enough δ, is

(c′) The diffeomorphisms Φ_i can be chosen, now possibly depending on η, so that each sphere Φ_i $(S^2 \times \{t\})$ has constant mean curvature $H_i(t)$, and that each H_i is a monotone function on $[-1, 1]$ with values in some interval $[-h(\eta), h(\eta)]$, where $h(\eta) > 2$.

To see that the initial data sets of section 2.3 have CMC foliations on each neck region, one can argue as follows. The quantitative estimates for the metric g_η on these neck regions from [21, section 8] show that if we scale (A_i, g_η) to have a fixed neck size (e.g., to have injectivity radius always equal to 1), then this annulus is C^2 quasi-isometric, with constant tending quickly to 1 as $\eta \to 0$, with the neck region for the Riemannian Schwarzschild space (scaled to have the same normalization). This latter space has a global CMC foliation, and by the implicit function theorem we can produce such a CMC foliation in any fixed neighbourhood of the neck. The outermost leaves of this foliation will have mean curvature $\pm h$, say, and when rescaled down to the original size, these leaves now have mean curvature $\pm h(\eta)$, where $h(\eta) \to \infty$.

We use this CMC foliation as follows. Consider the component $S_{i,\eta} = S_\eta \cap A_i$. Choose τ' and τ'' so that $S_{i,\eta} \subset S^2 \times [\tau', \tau'']$, and such that this is the narrowest band with this property. Then $S_{i,\eta}$ is tangent to both boundaries, and its outward unit normal at these points lies in the same direction as ∂_t. Denoting by H' and H'' the constant mean curvatures of those two boundaries, then the maximum principle gives that $H' \geqslant -2 \geqslant H''$. But $\tau' \leqslant \tau''$ and so $H' = H''$ and finally $S_{i,\eta}$ must coincide with a leaf of the foliation, and hence is connected.

4. Sections of event horizons have at least *I* components

In this section, we analyse the global structure of the maximal globally hyperbolic developments of families of initial data sharing certain overall properties with those of section 2.2, when the mass parameters are sufficiently small. This question is rather different from the one raised in the previous section, because the existence of apparent horizons involves only the geometry of the initial data, which is fairly well controlled. On the other hand, the notion of the event horizon involves the global structure of the resulting spacetime, about which only very scant information is available. Before proceeding further, the following should be said: because gravity is attractive, and because the Schwarzschild regions of the initial data of section 2.2 are initially at rest with respect to each other, one expects that those regions will

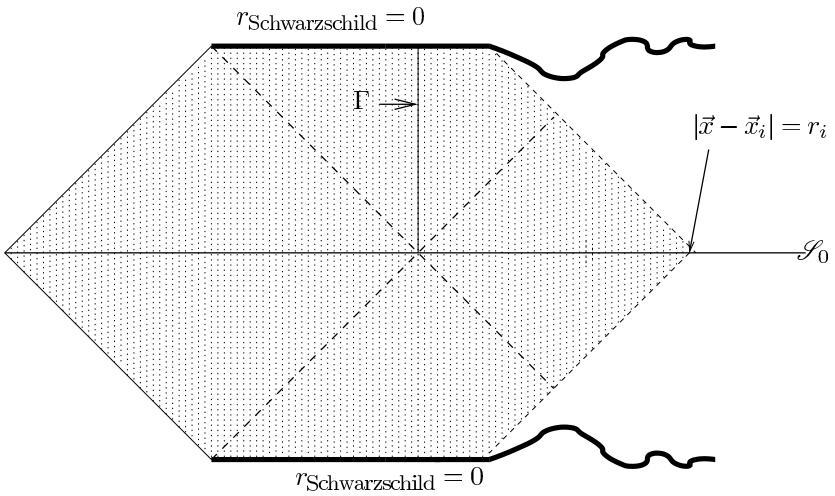

Figure 1. The maximal globally hyperbolic development of the initial data of section 2.2 in a neighbourhood of $B(\vec{x}_i, r_i)$. The metric in the dotted region is *exactly* the Schwarzschild metric. The 45° sloped dashed lines correspond to the Schwarzschild event horizons. The straight part of the boldface lines is *exactly* the Schwarzschild singularity; one expects that some form of that singularity will survive in nearby regions influenced by the non-Schwarzschildian initial data, as depicted by the curved part of the boldface line, but no results of this kind are known.

'start moving towards each other', leading either to the formation of naked singularities, or to a single black hole. In particular, the resulting event horizon, if occurring, is expected to be a connected hypersurface in spacetime. Nevertheless, the properties of the maximal globally hyperbolic developments $(\mathscr{M}, g)$ of the data which we present below lead us to conjecture that *there exists no slicing of $\mathscr{M}$ by Cauchy surfaces $\mathscr{S}_\tau$ which are asymptotically flat in all their asymptotic regions and in which all the intersections $\mathscr{E}^+ \cap \mathscr{S}_\tau$ are connected*. This seems to be the proper way of making precise the many-black-hole character of certain families of black-hole spacetimes. While we do not prove such a conjecture, it follows from what is said below that for some configurations there exist natural slicings of $\mathscr{M}$ which do have this property.

Recall that the black-hole event horizon $\mathscr{E}^+$ is usually defined as

$$\mathscr{E}^+ := \dot{J}^-(\mathscr{I}^+; (\tilde{\mathscr{M}}, \tilde{g})). \tag{4.1}$$

Here the causal past J^- is taken with respect to the conformally rescaled spacetime metric $\tilde{g}$ on the completed spacetime with boundary $\tilde{\mathscr{M}} := \mathscr{M} \cup \mathscr{I}^+$. Thus, the starting point of any black-hole considerations is the existence of a conformal completion at future null infinity $\mathscr{I}^+$. In this context, one usually assumes that $\mathscr{I}^+$ satisfies various completeness conditions [18, 19, 33] (compare the discussion in [8, 11]). As already mentioned, for the metrics of section 2.2 past-completeness of $\mathscr{I}^+$ is guaranteed by the fact that the initial data are exactly Schwarzschild outside of a compact set. However, the current understanding of the global properties of solutions of the Cauchy problem for the Einstein equations is insufficient to guarantee any future-completeness properties of the resulting $\mathscr{I}^+$. Nevertheless, we shall see that for some of those metrics the conformal boundary $\mathscr{I}^+$ can be chosen sufficiently large to the future so that $\mathscr{E}^+_{\mathscr{I}}$ defined by (1.1) will have more than one component. (This feature will persist upon enlarging $\mathscr{I}^+$, and will, therefore, also hold for a maximal one.) Before passing to a proof of this fact let us point out that the existence time of the solution,

defined as the lowest upper bound on the existence time of all geodesics normal to $\mathscr{S}$, goes to zero as the mass parameters go to zero. In order to see that, let Γ be a maximally extended future-directed timelike geodesic normal to $\mathscr{S}$ starting at the minimal neck of the Einstein–Rosen bridge of the usual Kruskal–Szekeres extension $(\mathscr{M}_{\text{Schw}}, g_{\text{Schw}})$ of the Schwarzschild spacetime with mass m. Either an explicit calculation, or a simple scaling argument, shows that the Lorentzian length of Γ is proportional to m. Now, if δ in (2.5) is small enough, then the maximal globally hyperbolic development $(\mathscr{M}, g)$ of the initial data of section 2.2 will contain a region isometrically diffeomorphic to a neighbourhood of Γ in $(\mathscr{M}_{\text{Schw}}, g_{\text{Schw}})$ as in figure 1. This shows that for small data $(\mathscr{M}, g)$ is necessarily 'small', in the sense made precise above, and a complete understanding of the global structure of the resulting spacetimes might be a delicate issue.

Let us return to the problem of main interest here, namely non-connectedness of sections of $\mathscr{E}^+_{\mathscr{S}}$, as defined by (1.1). We shall show that the stability results of Friedrich [16] can be used to reduce this question to elementary considerations of light-cones in Minkowski spacetime. Recall that the simplest conformal completion of the timelike future of a point in Minkowski spacetime $(\mathbb{R}^{3+1}, \eta)$ is obtained by performing the spacetime inversion

$$\{x^0 > 0, \eta_{\alpha\beta}x^\alpha x^\beta < 0\} \ni x^\mu \to y^\mu = \frac{x^\mu}{\eta_{\alpha\beta}x^\alpha x^\beta} \in \{y^0 < 0, \eta_{\alpha\beta}y^\alpha y^\beta < 0\}. \tag{4.2}$$

Here, $\eta_{\mu\nu}$ is the Minkowski metric. A drawback of transformation (4.2) is that it does not give the whole conformal completion of Minkowski spacetime at once; however, a major advantage thereof is that the rescaled metric is again the Minkowski one, so that the causal properties of the rescaled spacetime are straightforward to analyse, and to visualize:

$$\eta_{\mu\nu}\,\mathrm{d}x^\mu\,\mathrm{d}x^\nu = \frac{1}{(\eta_{\alpha\beta}y^\alpha y^\beta)^2}\eta_{\mu\nu}\,\mathrm{d}y^\mu\,\mathrm{d}y^\nu.$$

Under (4.2) the future timelike cone $I^+(0_x; (\mathbb{R}^{3+1}, \eta))$ of the origin 0_x of the x^μ coordinates becomes the past timelike cone $I^-(0_y; (\mathbb{R}^{3+1}, \eta))$ of the origin 0_y of the y^α coordinates; further, 0_y is the future timelike infinity point i^+, while $\dot{J}^-(0_y; (\mathbb{R}^{3+1}, \eta))$ becomes that part of the Minkowskian $\mathscr{I}^+$ which lies to the causal future of 0_x in the conformally completed Minkowski spacetime.

Choose, now, a set of points $\vec{y}_i$ and strictly positive numbers δ_i, $i = 1, \ldots, I$, with

$$|\vec{y}_i| + \delta_i < 1/2, \qquad \delta_i < |\vec{y}_i|, \tag{4.3}$$

with the balls $B(\vec{y}_i, \delta_i)$—pairwise disjoint. The points $\vec{y}_i$ should be thought as the y-coordinate equivalents of the points $\vec{x}_i$ of section 2.2. Let the initial surface $\mathscr{S}_0$ be defined by the equation[9]

$$\mathscr{S}_0 = \left\{y^0 = -\tfrac{1}{2}, 0 \leqslant |\vec{y}| < \tfrac{1}{2}, \vec{y} \notin B(\vec{y}_i, \delta_i)\right\} \tag{4.4}$$

with $(y^\mu) = (y^0, \vec{y})$. Set

$$\begin{aligned} K_i &:= \left\{y^0 = -\tfrac{1}{2}, \vec{y} \in B(\vec{y}_i, \delta_i)\right\}, \\ \mathscr{M}_\tau &:= \left\{-\tfrac{1}{2} \leqslant y^0 \leqslant \tau\right\} \cap I^-(0_y; (\mathbb{R}^{3+1}, \eta))\Big\backslash\Big(\cup_{i=1}^I J^+(K_i; (\mathbb{R}^{3+1}, \eta))\Big), \\ \tilde{\mathscr{M}}_\tau &:= \left\{-\tfrac{1}{2} \leqslant y^0 \leqslant \tau\right\} \cap J^-(0_y; (\mathbb{R}^{3+1}, \eta))\Big\backslash\Big(\cup_{i=1}^I J^+(K_i; (\mathbb{R}^{3+1}, \eta))\Big). \end{aligned} \tag{4.5}$$

[9] The value $-1/2$ for y^0 is chosen for definiteness; any other value can of course be chosen. It is, nevertheless, worthwhile mentioning that this choice corresponds to an upper hyperboloid $\{x^0 = -1 + \sqrt{1 + r^2}\}$. It appears that initial data similar to those of section 2.2 can be constructed directly on such hyperboloids by extending the techniques of Corvino and Schoen to a hyperboloidal setting.

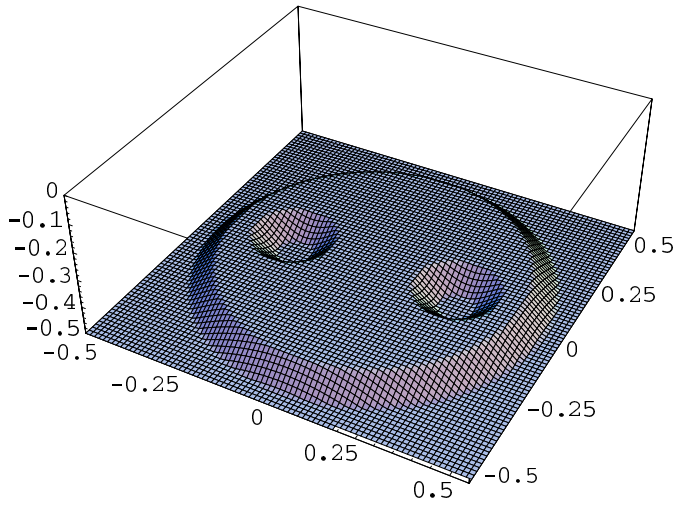

Figure 2. A $(2+1)$-dimensional version of the spacetime $\mathscr{M}_\tau$, $I = 2$, for τ smaller than the time τ_- of (4.7).

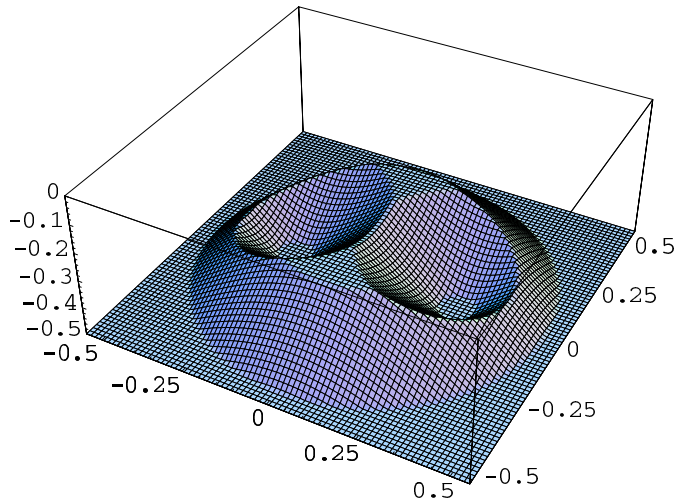

Figure 3. The spacetime $\mathscr{M}_\tau$ of figure 2 for $\tau_* < \tau < \tau_+$, with τ_* given by (4.8); compare figure 5.

(See figures 2–4.) The parameter τ should be thought of as the y^0-coordinate height of the regions on which the solution associated with the nontrivial initial data exists. One can think of the regions $J^+(K_i; (\mathbb{R}^{3+1}, \eta))$ as the regions where the nontrivial geometry, associated with neighbourhoods of the black-hole regions, is localized.

In order to take advantage of Friedrich's stability results [16], we make the following hypotheses: we consider families of hyperboloidal initial data sets $\{(g_\eta, K_\eta)\}_{\eta\in[0,\eta_0]}$, defined on $B\big(0, \frac{1}{2}\big)\setminus \cup_i \{\vec{y}_i\}_{i=1,\dots,I}$, for some $\eta_0 \in \mathbb{R}^+$, $I \in \mathbb{N}$, such that

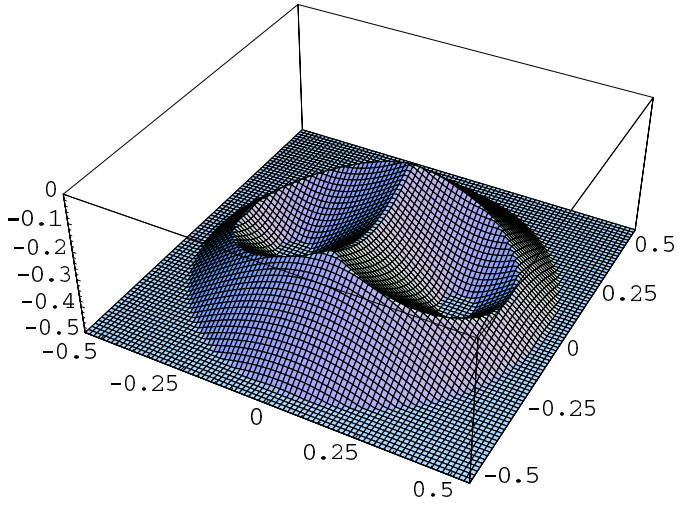

Figure 4. The spacetime $\mathscr{M}_\tau$ of figure 2 for τ larger than the time τ_+ of (4.9).

(a) *Uniform convergence.* For any open set $\mathscr{K}$ which has compact closure in $B(0, \frac{1}{2})\setminus \cup_i \{\vec{y}_i\}_{i=1,\dots,I}$ we have[10]

$$\lim_{\eta\to 0} \left(\|g_\eta - g_{\mathscr{H}}\|_{C^5(\mathscr{K})} + \|K_\eta - g_{\mathscr{H}}\|_{C^4(\mathscr{K})}\right) = 0.$$

Here $g_{\mathscr{H}}$ stands for the unit hyperbolic metric.

(b) *Existence of I trapped surfaces.* There exist $r_i, i = 1, \dots, I$ such that for every η there exists a compact smooth embedded trapped or marginally trapped surface $S_{i,\eta} \neq \emptyset$ satisfying

$$S_{i,\eta} \subset B(\vec{y}_i, r_i).$$

The balls $B(\vec{y}_i, r_i)$ will further be required to be pairwise disjoint. In some of the arguments below (b) will need to be strengthened to:

(b′) Moreover,

$$\limsup_{\eta\to 0}\{|\vec{y} - \vec{y}_i| : \vec{y} \in S_{i,\eta}\} = 0.$$

(For marginally trapped surfaces this does follow from (a), (b) and from what is said at the end of section 3.)

(c) *Existence of $\mathscr{I}^+$.* The resulting family of spacetimes admit conformal completions which are sufficiently differentiable so that Friedrich's stability theorem (or perhaps some extension thereof, in the spirit of [12, 29]) applies.

It is not immediately clear whether the initial data of section 2.2 are compatible with those hypotheses. There are a few issues here. Suppose, for instance, that the solution associated with the initial data of section 2.2 remains as close as desired to the Minkowski one, when making the mass parameters small, in a small neighbourhood of the spheres $S(\vec{x}_i, r_i)$, for a long time, and that the time in question tends to infinity as the mass parameters m_i go to zero. In such a case the hypotheses above would obviously hold, whatever the choice of the hyperboloidal initial surface $\mathscr{S}_0$. However, we are not aware of any argument which would

[10] The C^k norms here can be replaced by any Sobolev norms which guarantee that the resulting spacetime metric, obtained by evolving the initial data using the vacuum Einstein equations, is C^2.

justify that this is the correct picture, and the discussion around figure 1 suggests that this might actually be wrong. A simple way of avoiding the question of the time of existence of the solution near the spheres $S(\vec{x}_i, r_i)$ is to suppose that all the points $\vec{x}_i$ lie on the surface of some sphere[11]. We can then choose the hyperboloid so that the $\vec{x}_i$ lie on the intersection of this hyperboloid with the hypersurface $x^0 = 0$. For such configurations clearly all the hypotheses above are satisfied.

In this context, the following comment is also appropriate: so far we have assumed that the initial data are prescribed on the hypersurface $\mathscr{S}_0$ given by (4.4). The exact choice of $\mathscr{S}_0$ is clearly irrelevant, and a similar picture would be obtained at this stage with any hypersurface $\mathscr{S}_0$ which asymptotically approaches a hypersurface of constant conformal time y^0. In particular, we could choose $\mathscr{S}_0$ to coincide with the hypersurface $\{x^0\} = \text{const}$ for some large positive constant for $|\vec{y}| < R$, and to coincide with the hypersurface $\{y^0 = -1/2\}$ for $|\vec{y}|$ large enough. On $\mathscr{S}_0$, we can use the initial data of section 2.2 for $|\vec{y}| < R$, and appropriate data obtained by time evolution elsewhere. In such a case, the nature of the initial data of section 2.2 would guarantee that the induced data on the new hypersurface would have almost all the properties used in the discussion above: the only property missing is that the limiting data set, as η tends to zero, would not be the hyperbolic data set ($g = g_{\mathscr{H}}$, $K = g_{\mathscr{H}}$), but one corresponding to an appropriate hypersurface in Minkowski spacetime. However, our proof of existence of I components of the initial section of the event horizons relies on the fact that the radii δ_i can be made arbitrarily small on a hypersurface of constant y^0-time, and we would not be able to achieve the desired conclusions on general hypersurfaces.

Finally, consider the initial data of section 2.3 on asymptotically flat hypersurfaces and on hyperboloids; those initial data can be chosen to satisfy conditions (a), (b) and (b′) above. The initial data of [21] on asymptotically flat hypersurfaces are not known to satisfy condition (c). However, those constructed in [21] on hyperboloids can be chosen to satisfy that condition: the resulting globally hyperbolic developments will not have a $\mathscr{I}^+$ which is complete to the past, but it should be clear from the arguments below that this is irrelevant to most of the problems discussed here.

Returning to our model spaces $\mathscr{M}_\tau$, the corresponding model data on $\mathscr{S}_0$ are exactly those for the Minkowski metric. In the physical metric, the initial data on $\mathscr{S}_0$ will be close to the Minkowskian ones, the difference being as small as desired when η is made sufficiently small. Under conditions (a) and (c) as spelled out at the beginning of this section, the usual arguments about continuous dependence of solutions of hyperbolic PDEs upon initial data over compact sets, as applied to the conformal Einstein equations of Friedrich [16], show that for any fixed τ the physical metric g will exist on $\mathscr{M}_\tau$ and will be as close as desired to the Minkowski one on $\tilde{\mathscr{M}}_\tau$, when the initial data on $\mathscr{S}_0$ are sufficiently close to the Minkowski ones. This implies that the causal structure of the physical spacetime on $\tilde{\mathscr{M}}_\tau$ will be approximated as accurately as desired by that of the Minkowski spacetime on $\tilde{\mathscr{M}}_\tau$, when the initial data are sufficiently close to the Minkowskian ones on $\mathscr{S}_0$. In particular, the figures presented here will accurately describe the geometry of null geodesics in the physical spacetime.

Let

$$\mathscr{I}^+_\tau := \left\{-\tfrac{1}{2} \leqslant y^0 \leqslant \tau\right\} \cap \dot{J}^-(0_y; (\mathbb{R}^{3+1}, \eta)) \tag{4.6}$$

be the conformal boundary of $\mathscr{M}_\tau$ and suppose that

$$\tau < \tau_- := -\tfrac{1}{2} + \min_i \left|\tfrac{1}{2} - |\vec{y}_i| - \delta_i\right|. \tag{4.7}$$

[11] This involves no loss of generality if $I = 2$, or if $I = 3$ and the $\vec{x}_i$ are not aligned. However, for $I = 3$ the configurations of section 2.2 are actually co-linear.

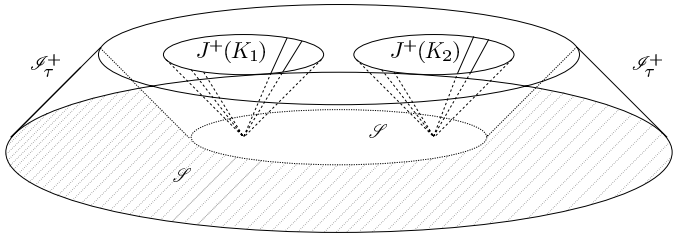

Figure 5. $\tilde{\mathscr{M}}_\tau$ for $\tau < \tau_-$, compare figure 2. The shaded area is the part of $\mathscr{S}$ which can be seen from $\mathscr{I}^+_\tau$, and its complement in $\mathscr{S}$ is therefore the (partly 'physically wrong') black-hole region, within $\mathscr{S}$, with respect to $\mathscr{I}^+_\tau$.

In that case, the black-hole event horizon $\mathscr{E}^+_\tau$, in the spacetime $(\tilde{\mathscr{M}}_\tau, \eta)$, associated with the conformal boundary $\mathscr{I}^+_\tau$,

$$\mathscr{E}^+_\tau := \dot{J}^-\big(\mathscr{I}^+_\tau; (\tilde{\mathscr{M}}_\tau, \eta)\big),$$

will be a union of spheres:

$$\mathscr{E}^+_\tau = \cup_{t\in[-\frac{1}{2},\tau]}\{y^0 = t, |\vec{y}| = -2\tau + t\},$$

see figure 5. In particular, $\mathscr{E}^+_\tau$ will be connected, so that each section thereof through a hypersurface

$$\{y^0 = \text{const}\}$$

will also be connected. This holds for the Minkowski metric, and hence also for the physical metric for initial data sufficiently close to Minkowskian ones. Thus, if the physical spacetime develops a singularity and stops to exist at some time τ satisfying (4.7), then the boundary of the black-hole region will be connected. As long as this last possibility occurs it is meaningless—within the $\mathscr{I}^+$ framework—to assert that $\mathscr{M}_\tau$ is a multi-black-hole spacetime[12]. We stress that the global structure of figure 5 could very well arise for nontrivial initial data, whether small or large, *even if all singularities are shielded by the event horizon* (in which case τ, near $\mathscr{I}^+$, can be thought of as being infinite, and should not be identified with a Minkowskian coordinate). The point of our considerations below is to show that this will not happen for some configurations.

Now, as soon as the initial value of y^0 exceeds the value τ_- given by (4.7), some null geodesics starting with this initial value backwards in time from the Minkowskian Scri

$$\mathscr{I}^+_{(\mathbb{R}^{3+1},\eta)} := \dot{J}^-(0_y; (\mathbb{R}^{3+1}, \eta))$$

enter the region $J^+(K_i)$ where the metric fails to be close to the Minkowski one, even for small mass positive parameters m_i, and where singularities *do* form in a short time. The visibility of those singularities from $\mathscr{I}^+$ would be forbidden if a suitable version of the cosmic censorship hypothesis is applied, but no such results have been established so far. As of today there is no justification for the possibility that the physical $\mathscr{I}^+$ can be continued uniformly beyond the points at which some of the generators of the Minkowskian $\mathscr{I}^+$ meet some null geodesics emanating from the K_i (though these generators actually do continue 'a little' in the situation at hand). Whatever the case, stability implies that one might continue with each generator of

[12] On the other hand, at an intuitive level it is clear that, whatever the value of τ, the physical spacetime does contain distinct regions which display 'black-hole' properties, even though this does not fit well into the $\mathscr{I}$ framework. It seems that any significant insight into such situations will be gained only after a better understanding of the long-time behaviour of solutions of Einstein equations is reached.

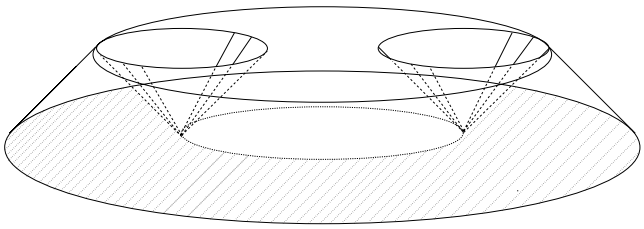

Figure 6. $\tilde{\mathscr{M}}_\tau$ with $\tau = \tau_-$. The shaded area is the part of $\mathscr{S}$ which can be seen from $\mathscr{I}^+_\tau$.

the physical $\mathscr{I}^+$, associated with the nontrivial initial data, to the future from the boundary of the initial data hypersurface *up to the first point* the Minkowskian past of which intersects one of the K_i. From this point of view the only significant feature distinguishing various values of τ is that sections of the model $\mathscr{I}^+_\tau$, as defined by (4.6), with hypersurfaces $\{y^0 = t\}$ will be spheres for $t < \tau_-$, cf figures 2 and 5, while this will not be the case anymore if $\tau > t > \tau_-$. Furthermore, the causal geometry of $(\tilde{\mathscr{M}}_\tau, \eta)$ becomes interesting only for

$$\tau > \tau_* := -\tfrac{1}{2} + \min_i \left|\tfrac{1}{2} - |\vec{y}_i| + \delta_i\right|. \tag{4.8}$$

We shall not attempt to analyse exhaustively what happens for all $\tau > \tau_*$ and all possible values of $\vec{y}_i$, but we will concentrate on a few specific cases. We set

$$\mathscr{E}^+_\tau(0) := \mathscr{E}^+_\tau \cap \mathscr{S}_0.$$

We wish to exhibit configurations for which $\mathscr{E}^+_\tau(0)$ has at least I components. Now, by standard causality theory[13], the $S_{i,\eta}$ of condition (b) cannot be seen from $\mathscr{I}^+_\tau$, whatever the value of τ (see figure 6). It follows that $\mathscr{E}^+_\tau(0)$ is never empty. Our aim is to construct hypersurfaces $\mathscr{N}_i \subset \mathscr{S}_0$, $i = 1, \ldots, I-1$, with the following properties.

1. $\mathscr{N}_i \subset I^-\left(\mathscr{I}^+_\tau\right)$, so that $\mathscr{E}^+_\tau(0) \cap \mathscr{N}_i = \emptyset$.
2. The $\mathscr{N}_i$ separate $\mathscr{S}_0$ into I distinct, open, connected sets $\mathscr{O}_i$ such that each $\mathscr{O}_i$ contains precisely one $S_{i,\eta}$.

It then clearly follows that $\mathscr{E}^+_\tau(0)$ has at least I components.

Let us start with the case $I = 2$. Without loss of generality one can then assume $\vec{x}_1 = -\vec{x}_2$. Further, under the current hypotheses one can, without loss of generality, assume that the constants δ_i of (4.3) satisfy $\delta_1 = \delta_2$ by replacing the smaller of the δ_i by the larger one, and making the parameter η smaller if necessary. From now on we assume that η has been chosen small enough so that the physical metric exists on $\mathscr{M}_\tau$ with τ larger than

$$\tau_+ := a^2 - \tfrac{1}{4} < 0. \tag{4.9}$$

This value of τ corresponds to the value of y^0 at the meeting points of a generator of $\dot{J}^+(K_1, (\mathbb{R}^{3+1}, \eta))$ *and* a generator of $\dot{J}^+(K_2, (\mathbb{R}^{3+1}, \eta))$ *and* a generator of $\dot{J}^-(0_y, (\mathbb{R}^{3+1}, \eta))$ —see the proof of proposition 4.1. This is also the 'highest point' of $\mathscr{M}_\tau$ for $\tau \geqslant \tau_+$, compare figures 4, 7 and 8. Finally, this corresponds to the value of τ above which $\mathscr{M}_\tau$ does not change any more:

$$\forall\, \tau \geqslant \tau_+ \quad \mathscr{M}_\tau = \mathscr{M}_{\tau_+}.$$

It is then obvious from figure 7, in which the K_i are very close to the conformal boundary, that the past of the 'highest points' of $\mathscr{M}_\tau$ contains points lying on the straight line segment

[13] In the case of the initial data of section 2.2 the use of causal theory is actually not needed: the existence of black-hole regions follows immediately from the Schwarzschildian character of the data on $B(x_i, r_i)$, as made clear by figure 5.

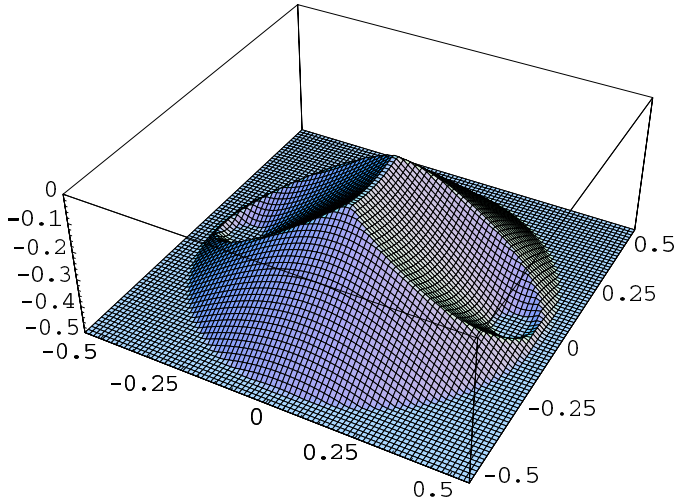

Figure 7. M_0 for $\vec{y}_i$ close to the conformal boundary.

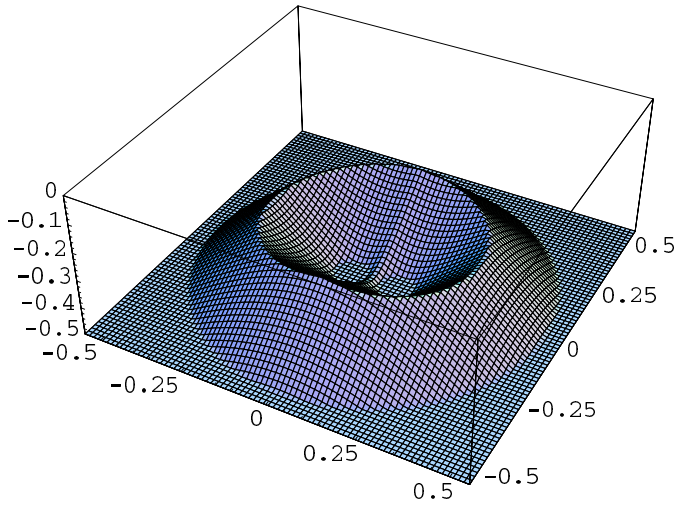

Figure 8. M_0 for $\vec{y}_i$ close to each other.

connecting the two black holes. This same property is still visible, though with a little more effort, from figure 4 where the black-hole regions are fairly far away from each other. On the other hand, it should be clear from figure 8 that $\mathscr{E}^+_{\tau_+}(0)$ will be connected there. Before presenting a precise form of those statements, let us introduce the notation

$$(y^\mu) = (t, x, y, z).$$

In the proposition that follows the constant $-1/2$ appearing in (4.4) and (4.5), representing the y^0 coordinate of the initial data hypersurface, has been replaced by an arbitrary constant $\tau_0 < 0$.

Proposition 4.1. *Suppose that* $I = 2, \delta := \delta_1 = \delta_2, \vec{y}_1 = -\vec{y}_2$, *set* $a := |\vec{y}_1|$. *Then the plane*

$$\mathscr{N}_1 := \{t = \tau_0, x = 0\} \subset \{t = \tau_0\}$$

is included in $J^-\big(\mathscr{I}^+_{\tau_+}, (\tilde{\mathscr{M}}_{\tau_+}, \eta)\big)$ *if and only if*

$$\frac{2\delta}{|\tau_0|} \leqslant \sqrt{1+\left(\frac{2a}{|\tau_0|}\right)^2} - 1. \tag{4.10}$$

Remark 4.2. Equations (4.10) always hold for small enough $\delta/|\tau_0|$. This is all that is needed for our purposes: the sets K_i have been chosen to contain the nontrivial geometry, and condition (a) guarantees that they can be chosen as small as desired by choosing the parameter η small enough. On the other hand, it *is* restrictive: for example, for $a/|\tau_0| = 1/2$, which is the case in figures 3 and 4, (4.10) leads to $\delta \leqslant (\sqrt{2}-1)|\tau_0|/2$. This last inequality can be violated by an appropriate choice of δ compatible with our remaining restrictions $\delta < a$, $\delta + |a| < |\tau_0|$.

Proof. Clearly $p_0 := (\tau_0, \vec{0}) \in J^-\big(\mathscr{I}^+_{\tau_+}\big)$ if and only if the whole plane $\{t = \tau_0, x = 0\}$ is included in $J^-\big(\mathscr{I}^+_{\tau_+}\big)$ (throughout this proof all the causal objects are taken in $(\mathbb{R}^{3+1}, \eta)$). Set $p_i = (\tau_0 - \delta, \vec{y}_i)$, then

$$J^+(K_i) = J^+(p_i) \cap \{t \geqslant \tau_0\}.$$

Without loss of generality we may assume $\vec{x}_1 = (a, 0, 0)$. A simple calculation gives

$$\dot{J}^+(K_1) \cap \dot{J}^+(K_2) \cap \dot{J}^-(0_y) = \big\{(\tau_\delta, 0, y, z) \mid y^2 + z^2 = \tau_\delta^2\big\} \subset \{x = 0\},$$

with

$$\tau_\delta := \frac{a^2 - (|\tau_0| + \delta)^2}{2(|\tau_0| + \delta)} < 0.$$

On the other hand,

$$\dot{J}^+(p_0) \cap \dot{J}^-(0_y) \cap \{x = 0\} = \left\{ \left(\frac{\tau_0}{2}, 0, y, z\right) \middle| \, y^2 + z^2 = \left(\frac{\tau_0}{2}\right)^2 \right\}.$$

It then easily follows, e.g., by symmetry arguments, that p_0 will be in the causal past of $\mathscr{I}^+_{\tau_+}$ if and only if

$$\frac{\tau_0}{2} \leqslant \tau_\delta.$$

This last equation is equivalent to (4.10). □

Proposition 4.1 together with remark 4.2 settles the case $I = 2$. In order to proceed further, it is necessary to understand the geometry of the intersections

$$\dot{J}^+(p) \cap \dot{J}^-(0_y), \qquad p \in I^-(0_y).$$

It is convenient to consider general spacetime dimensions $n + 1$. Let $\tau_0 < 0$ and let $p = (\tau_0, \vec{q}) \in I^-(0) \subset \mathbb{R}^{n+1}$, with $\vec{q} \in B(0, |\tau_0|) \subset \mathbb{R}^n$; for the discussion here all the causal objects are defined with respect to the Minkowski metric η in $\mathbb{R}^{n+1}$. We denote by π the projection along the first, timelike coordinate axis in $\mathbb{R}^{n+1}$ (associated with a coordinate which we denote by x^0). We set

$$\mathscr{U}_{\vec{q}} := J^+((\tau_0, \vec{q})) \cap \dot{J}^-(0), \qquad \mathscr{O}_{\vec{q}} := \pi(\mathscr{U}_{\vec{q}}).$$

A simple computation shows that the $\mathscr{O}_{\vec{q}}$ are solid ellipsoids: for $\vec{q} = (a, \vec{0})$, $|a| < |\tau_0|$, where $\vec{0}$ denotes the origin in $\mathbb{R}^{n-1}$, we have

$$\mathscr{O}_{(a,\vec{0})} = \left\{ \left(x - \frac{a}{2}\right)^2 + \frac{\rho^2}{1 - \frac{a^2}{|\tau_0|^2}} \leqslant \left(\frac{\tau_0}{2}\right)^2 \right\}, \qquad \rho^2 := (x^2)^2 + \cdots + (x^n)^2. \tag{4.11}$$

Here, we use the symbol x to denote the first coordinate in $\mathbb{R}^n$. For further purposes, the following properties of the $\mathscr{O}_{(a,\vec{0})}$ are useful.

- The $\mathscr{O}_{(a,\vec{0})}$ are all cigar shaped, except for the one with $a = 0$ which is a ball of radius $|\tau_0|/2$.
- The $\mathscr{O}_{(a,\vec{0})}$ are centred at $(a/2, \vec{0})$, and their extent in the first coordinate x equals τ_0, independently of a.
- The intersection of the $\mathscr{O}_{(a,\vec{0})}$ with the central hyperplane $\{x = a/2\}$ is an $(n-1)$-dimensional ball of radius $f(a/|\tau_0|)$, where $f(\beta) = |\tau_0|\sqrt{1-\beta^2}/2$. The function $f : [0, 1] \to [0, |\tau_0|/2]$ is strictly decreasing.
- We further have

$$(\partial\mathscr{O}_{(a,\vec{0})}) \cap \{x = a/2\} \subset S^{n-1}(0, |\tau_0|/2) \subset \mathbb{R}^n; \tag{4.12}$$

we have decorated the sphere $S^{n-1}(0, |\tau_0|/2)$ with a subscript $n-1$ to emphasize its dimension. The sections (4.12) are the 'fattest' x-sections of the $\mathscr{O}_{(a,\vec{0})}$. Thus, as a increases from 0 to $|\tau_0|$ the fattest part of $\mathscr{O}_{(a,\vec{0})}$ thins out, with its boundary travelling on $S^{n-1}(0, |\tau_0|/2)$ from the equatorial hyperplane $\{x = 0\}$ all the way to the north pole $x = |\tau_0|/2$. The ellipsoids degenerate to a line in this last limit.

The following simple rules complement the above properties.

1. Let $\vec{x} \in B^n(0, |\tau_0|)\backslash\mathscr{O}_{(a,\vec{0})}$. Then the point $p = (\tau_0, \vec{x})$ is in the timelike past of

$$\dot{J}^-(0)\backslash I^+((\tau_0, a, \vec{0}));$$

the required timelike curve is simply a segment of the vertical line $t \to (t, \vec{x})$.

2. If $\vec{x} \in (\partial\mathscr{O}_{(a,\vec{0})}) \cap \pi\big(\mathscr{I}^+_\tau\big)$, then the whole line segment $s(a, \vec{0}) + (1-s)\vec{x}, s \in (0, 1)$ is included in $I^-\big(\mathscr{I}^+_{\tau_+}\big)$. Indeed, by the definition of $\mathscr{O}_{(a,\vec{0})}$ there exists a causal geodesic Γ from $(a, \vec{0})$ to a point p on $\mathscr{I}^+_\tau$, with p projecting down to $\vec{x}$—the projection $\pi(\Gamma)$ of Γ is the line segment $s(a, \vec{0}) + (1-s)\vec{x}, s \in [0, 1]$. The required timelike curve is obtained by a timelike deformation of the following path: one first moves from $(\tau_0, \vec{x})$ towards the future along the x^0 coordinate line until one meets Γ, and then one moves along Γ until one meets $\mathscr{I}^+_\tau$. We note that if p is not on an edge of $\mathscr{I}^+_\tau$, then the whole closed segment $s(a, \vec{0}) + (1-s)\vec{x}, s \in [0, 1]$, will actually be included in $I^-\big(\mathscr{I}^+_\tau\big)$.

We consider now the case of three or more K_i. The simplest configuration is that with all the points $\vec{y}_i$ aligned; without loss of generality we can then assume that they lie on the axis $\{y = z = 0\}$. We have the following result, where we do not assume $I = 3$ (see figure 9).

Theorem 4.3. *Suppose that all the $\vec{y}_i$ are co-linear, and that the hypotheses (a), (b), (b′) and (c) of the beginning of this section hold. Then for η small enough $\mathscr{E}^+_{\tau_+}(0)$ has at least I components.*

Proof. The case $I = 2$ is covered by proposition 4.1, it is thus sufficient to consider $I \geqslant 3$. We will construct hypersurfaces $\mathscr{N}_i$ which will be included in $I^-\big(\mathscr{I}^+_{\tau_+}\big)$ for $\delta_i = 0$, as all the objects involved depend continuously upon δ_i the result for small δ_i will follow.

Consider first the case of space dimension $n = 2$, let $\vec{y}_i = (a_i, 0)$. Then

$$\pi\big(\mathscr{I}^+_{\tau_+}\big) = B(0, |\tau_0|)\backslash\cup_i \mathscr{O}_{(a_i,0)}.$$

Suppose that $I = 3$, without loss of generality we may assume $a_1 > 0$, consider any point $b \in (0, a_1)$. What has been said concerning the geometry of the $\mathscr{O}_{(a,\vec{0})}$ implies that the set

$$\mathscr{V}_b := \big\{\mathscr{O}_{(b,0)} \cap \pi\big(\mathscr{I}^+_{\tau_+}\big)\big\} \cap \{x \geqslant 0\} = \big\{\mathscr{O}_{(b,0)}\big\backslash\big\{B(0, |\tau_0|/2) \cup \mathscr{O}_{(a_1,0)}\big\}\big\} \cap \{x \geqslant 0\}$$

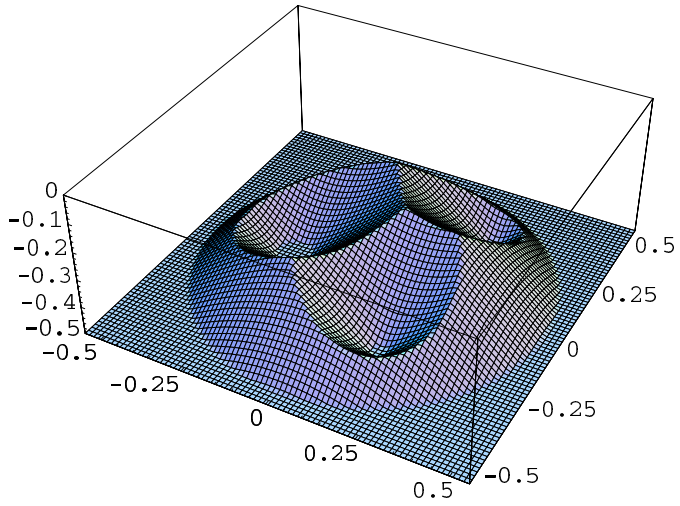

Figure 9. A (2 + 1)-dimensional version of the spacetime $\mathscr{M}_\tau$, $I = 3$, for τ sufficiently large.

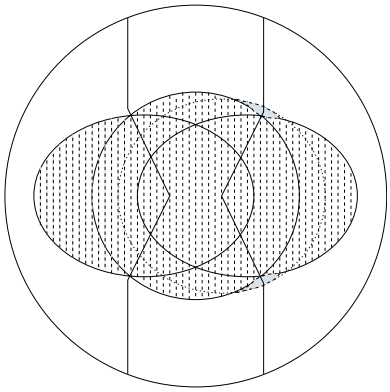

Figure 10. Three black holes, aligned. The outermost circle represents the conformal boundary of $\mathscr{I}_0$. The dotted region is the projection on the initial hypersurface $\mathscr{I}_0$ of the part of $\dot{J}(0_y)$ which has been excised by the removal of $J^+(K_1) \cup J^+(K_2)$. The shaded region is $\mathscr{V}_b$.

is non-empty; see figure 10. Since the dimension is two, the desired hypersurface $\mathscr{N}_1$ is actually a curve, obtained as follows: let $\vec{x}$ be any point in $\mathscr{V}_b$, let γ_1 be the segment $s\vec{x} + (1-s)(b, 0)$, $s \in [0, 1]$. Let γ_2 be the path obtained by first following γ_1, and then a line parallel to the y axis. By the rules (1) and (2) γ_2 is included in $I^-\left(\mathscr{I}^+_{\tau_+}\right)$. We define $\mathscr{N}_1$ to be the union of γ_2 and of its image under the map $(x, y) \to (x, -y)$. The second hypersurface $\mathscr{N}_2$ is obtained by taking the image of $\mathscr{N}_1$ under the map $(x, y) \to (-x, y)$.

It should be obvious to the reader how this construction generalizes to higher I. We simply note that for $I = 2N$ one of the curves, say $\mathscr{N}_N$, can always be chosen to be the axis $\{x = 0\}$. Figure 11 illustrates the case $I = 4$.

For dimensions $n \geqslant 3$ the desired hypersurfaces can be obtained by rotating the curves constructed above around the axis $\{y^2 = \cdots = y^n = 0\}$ using the action of $SO(n-1) \subset SO(n)$. □

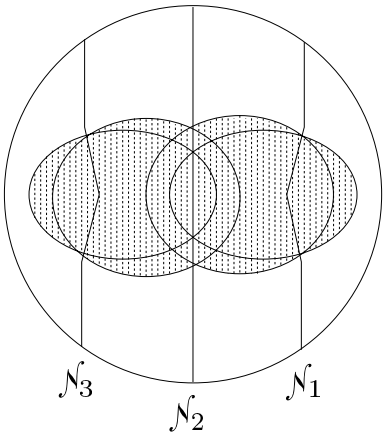

Figure 11. Four black holes, aligned. The dotted region is the projection on the initial hypersurface $\mathscr{S}_0$ of the part of $\dot{J}(0_y)$ which has been excised by the removal of $J^+(K_1) \cup J^+(K_2) \cup J^+(K_3)$.

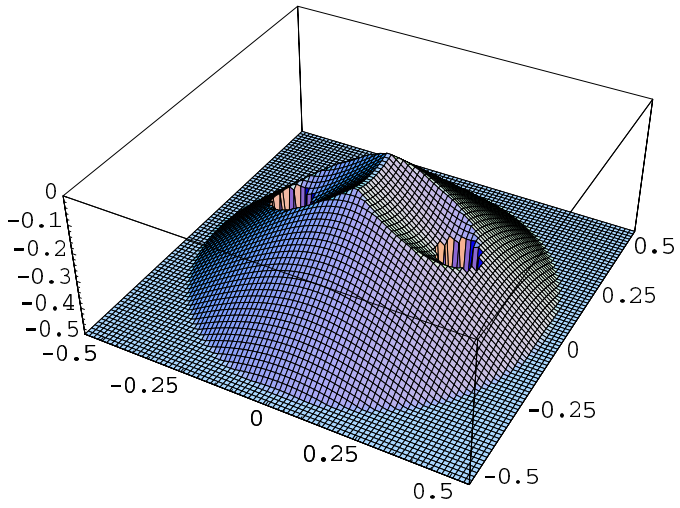

Figure 12. Two black holes, with the metric staying close to the Minkowski one near the spheres $S(\vec{x}_i, r_i)$ for a significant time.

Using our discussion of the geometry of the $\mathscr{O}_q$, with a little work the reader should be able to verify the following.

Theorem 4.4. *Let* $|\vec{n}_i| = 1$ *for all* i*, and let* $\vec{y}_i = \lambda \vec{n}_i$*. There exists* $0 < \lambda_0 < 1/2$ *such that for all* $\lambda_0 \leqslant \lambda < 1/2$ *the black-hole region* $\mathscr{E}^+_{\tau_+}(0)$ *has at least* I *components.*

One expects that there exist configurations with $I > 3$ for which $\mathscr{E}^+_{\tau_+}(0)$ has less than I components. While it is easy to imagine such configurations, a justification does not seem to be straightforward.

So far we have not been assuming anything about how long the metric remains close to the flat one in a small neighbourhood of the spheres $S(\vec{x}_i, r_i)$. The longer this happens, the larger the set of slices $\{y^0 = \tau\}$ at which the horizon has more than one component. This is made clear by figures 12 and 13.

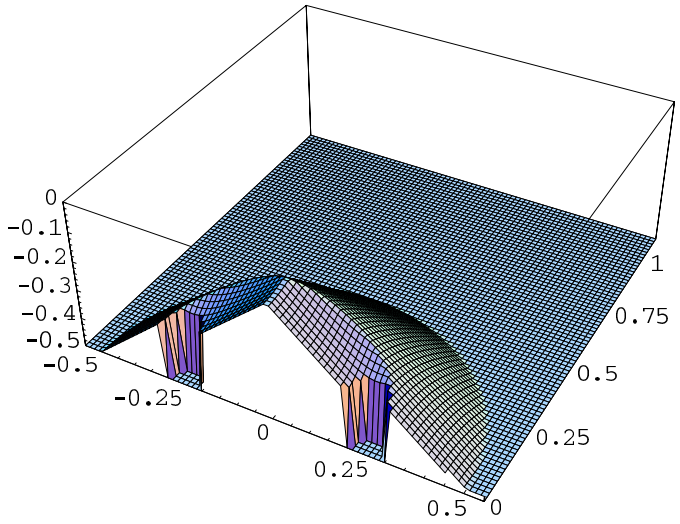

Figure 13. The part $y \geqslant 0$ of the spacetimes of figure 12.

5. Concluding remarks

We have exhibited one parameter families of initial data which contain non-connected outermost apparent horizons, as well as non-connected black-hole regions; here non-connectedness is understood in the sense of intersection of the black-hole region with the initial data surface. These examples are specific to the recently constructed families of initial data discussed in section 2, and we have not attempted to find general conditions which would ensure that this phenomenon occurs. Indeed, it is far from clear whether these families are truly representative of more general situations.

Both in numerical simulations, and when dealing with solutions obtained by analytical methods, it would be quite useful to have reasonably sharp criteria to check whether the initial data or spacetime under consideration contain disconnected black-hole regions. Since our argument concerning the outermost apparent horizon proceeded by contradiction, it gives no such criterion. It would be of considerable interest to find a quantitative version of this argument, leading to explicit estimates on the geometry which would guarantee this disconnectedness. Such estimates or criteria are not known even for the simplest and most explicit multi-black-hole initial data sets, i.e. those of Brill–Lindquist. Although one has non-connectedness in this case when the mass parameters are sufficiently small, we do not know any estimate on the 'connectedness threshold' if any.

The situation for black-hole regions on hyperboloidal hypersurfaces seems more tractable though. In this case, our analysis involved a reduction of the problem to straightforward considerations concerning the geometry of Minkowski spacetime, and leads to the following strategy, within a numerical framework based on the conformal field equations [15, 17]. Suppose one numerically evolves a candidate multi-black-hole configuration in a conformally completed spacetime. If the metric remains small, for a sufficiently long time, in a region determined by the Minkowskian analysis of the problem at hand, then the black-hole region in the associated spacetime will intersect the initial data hypersurface in a non-connected set. It is our understanding that this is far from practical at present since codes for the evolution of black holes tend to crash rather rapidly. However, it is generally expected that it will be

possible to perform long-time numerical evolutions of black-hole spacetimes in the not too distant future.

Acknowledgments

PTC acknowledges useful discussions with E Delay, G Galloway and R Schoen. He is grateful to the American Institute of Mathematics, Stanford University and the NSF for financial support at the Stanford Workshop on General Relativity during a part of the work on this paper. RM wishes to thank S Kerckhoff for a helpful conversation about 3-manifold topology. Thanks are due to J Chruściel and S Nicolis for helping with the computer-generated drawings. PTC was partially supported by a Polish Research Committee grant and RM was partially supported by NSF grant DMS-0204730.

References

[1] Alcubierre M, Brandt S, Brügmann B, Gundlach C and Massó J 2000 Test-beds and applications for apparent horizon finders in numerical relativity *Class. Quantum Grav.* **17** 2159–90 (*Preprint* gr-qc/9809004)

[2] Alcubierre M, Brugmann B, Pollney D, Seidel E and Takahashi T 2001 Black-hole excision for dynamic black holes *Phys. Rev.* D **64** 061 501 (*Preprint* gr-qc/0104020)

[3] Beig R 2000 Generalized Bowen–York initial data *Meeting Mathematical and Quantum Aspects of Relativity and Cosmology Proc. 2nd Samos Meeting (Lecture Notes in Physics vol 537)* ed S Cotsakis *et al* (Berlin: Springer) pp 55–69

[4] Beig R and Murchadha N Ó 1996 Vacuum spacetimes with future trapped surfaces *Class. Quantum Grav.* **13** 739–51

[5] Cai M and Galloway G J 2000 Rigidity of area minimizing tori in 3-manifolds of non-negative scalar curvature *Commun. Anal. Geom.* **8** 565–73

[6] Choi H I and Schoen R 1985 The space of minimal embeddings of a surface into a three-dimensional manifold of positive Ricci curvature *Invent. Math.* **81** 387–94

[7] Christodoulou D The global initial value problem in general relativity *Proc. 9th Marcel Grossman Meeting* webpage http://141.108.24.15:8000

[8] Chruściel P T 2002 Black holes *Proc. Tübingen Workshop on the Conformal Structure of Space-Times (Lecture Notes in Physics vol 604)* ed H Friedrich and J Frauendiener (Heidelberg: Springer) pp 61–102

[9] Chruściel P T and Delay E 2002 Existence of non-trivial asymptotically simple vacuum spacetimes *Class. Quantum Grav.* **19** L71–9 (*Preprint* gr-qc/0203053)
Chruściel P T and Delay E 2002 *Class. Quantum Grav.* **19** 3389 (erratum)

[10] Chruściel P T and Delay E 2002 On mapping properties of the general relativistic constraints operator in weighted function spaces, with applications *Preprint* gr-qc/0301073

[11] Chruściel P T, Delay E, Galloway G and Howard R 2001 Regularity of horizons and the area theorem *Ann. H Poincaré* **2** 109–78 (*Preprint* gr-qc/0001003)

[12] Chrusciel P T and Lengard O Solutions of Einstein equations polyhomogeneous at Scri (in preparation)

[13] Corvino J 2000 Scalar curvature deformation and a gluing construction for the Einstein constraint equations *Commun. Math. Phys.* **214** 137–89

[14] Dain S 2001 Initial data for two Kerr-like black holes *Phys. Rev. Lett.* **87** 121102 (*Preprint* gr-qc/0012023)

[15] Friedrich H 2002 Conformal Einstein evolution *Proc. Tübingen Workshop on the Conformal Structure of Space-Times (Lecture Notes in Physics vol 604)* ed H Friedrich and J Frauendiener (Heidelberg: Springer) pp 1–50

[16] Friedrich H 1986 On the existence of n–geodesically complete or future complete solutions of Einstein's field equations with smooth asymptotic structure *Commun. Math. Phys.* **107** 587–609

[17] Friedrich H 1998 Einstein's equation and geometric asymptotics *Gravitation and Relativity: At the Turn of the Millenium (Pune) (Proc. GR15)* ed N Dadhich and J Narlikar (IUCAA) pp 153–76

[18] Geroch R and Horowitz G 1978 Asymptotically simple does not imply asymptotically Minkowskian *Phys. Rev. Lett.* **40** 203–6

[19] Hawking S W and Ellis G F R 1973 *The Large Scale Structure of Space-Time* (Cambridge: Cambridge University Press)

[20] Huisken G and Ilmanen T 2001 The inverse mean curvature flow and the Riemannian Penrose inequality *J. Diff. Geom.* **59** 353–437 webpage http://www.math.nwu.edu/~ilmanen
[21] Isenberg J, Mazzeo R and Pollack D 2002 Gluing and wormholes for the Einstein constraint equations *Commun. Math. Phys.* **231** 529–68 (*Preprint* gr-qc/0109045)
[22] Isenberg J, Mazzeo R and Pollack D 2002 On the topology of vacuum spacetimes *Preprint* gr-qc/0206034 (*Ann. H Poincaré* to appear)
[23] Joyce D Constant scalar curvature metrics on connected sums *PhD Thesis* Lincoln College, Oxford (*Preprint* math.DG/0108022)
[24] Klainerman S and Nicolò F 1999 On local and global aspects of the Cauchy problem in general relativity *Class. Quantum Grav.* **16** R73–157
[25] Korevaar N J and Kusner R 1993 The global structure of constant mean curvature surfaces *Invent. Math.* **114** 311–32
[26] Korevaar N J, Kusner R, Meeks W H III and Solomon B 1992 Constant mean curvature surfaces in hyperbolic space *Am. J. Math.* **114** 1–43
[27] Lehner L 2001 Numerical relativity: status and prospects *Proc. GR16 (Durban, South Africa, 15-21 July 2001)* (*Preprint* gr-qc/0202055)
[28] Lehner L 2001 Numerical relativity: a review *Class. Quantum Grav.* **18** R25–86 (*Preprint* gr-qc/0106072)
[29] Lengard O Solutions of the Einstein's equation, wave maps, and semilinear waves in the radiation regime *PhD Thesis* Université de Tours 2001 http://www.phys.univ-tours.fr/~piotr/papers/batz
[30] Schoen R 1983 Estimates for stable minimal surfaces in three-dimensional manifolds *Semin. on Minimal Submanifolds, Ann. Math. Stud.* **103** 111–26
[31] Schoen R and Yau S-T 1979 Existence of incompressible minimal surfaces and the topology of three dimensional manifolds with non-negative scalar curvature *Ann. Math.* **110** 127–42
[32] Simon L 1983 Lectures on geometric measure theory *Proc. CMA* vol 3 (Canberra: Australian University Press)
[33] Wald R M 1984 *General Relativity* (Chicago: University of Chicago Press)
[34] Wald R M and Iyer V 1991 Trapped surfaces in the Schwarzschild geometry and cosmic censorship *Phys. Rev.* D **12** R3719–22
[35] Witten E and Yau S T 1999 Connectedness of the boundary in the AdS/CFT correspondence *Adv. Theor. Math. Phys.* **3** 1635–55 (*Preprint* hep-th/9910245)